

Research Article

Theoretical analysis of organic Rankine cycle for maximum power generation in optimization operation conditions

Baoju Jia^a, Yu Lei^b, Faming Sun^a, Weisheng Zhou^{c,*}^a Research Institute of Global 3E, Kyoto, Japan^b Dongfang Electric Engineering & Consulting Co., Ltd, China^c College of Policy Science, Ritsumeikan University, Japan

ARTICLE INFO

Keywords:

Theoretical analysis
Maximum power generation
Organic rankine cycle
R717
R134a
R1234yf
R290
R245fa
R1233zd
Optimization operation

ABSTRACT

The global critical issue in energy scarcity should be appropriately solved to realize a sustainable society. Effective use of Rankine cycle is one possible way since it provides most of worldwide electricity production. In this paper, theoretical analysis model of organic working fluids R717, R134a, R1234yf, R290, R245fa and R1233zd in Rankine cycle for maximum power generation in optimization operation using low-temperature heat sources are proposed and studied for development next generation green and zero-carbon energy generation system to promote the race to zero. Results show that temperatures of warm and cold water at inlet, mass flow rate of the warm water and performance of the evaporator play a key role to obtain the theoretical optimization operation conditions for maximum power generation. In the case of same initial conditions of temperatures of warm water (85°C) and cold water (15°C) at inlet, mass flow rate of the warm water (10 kg/s) and performance of the evaporator (100 kW/K), R717 has the best performance in terms of the maximum power output 56.0 kW with thermal efficiency of 8.6%, and the next is the R1233zd (54.4 kW, 8.3%), R245fa (54.0 kW, 8.2%), R134a (52.8 kW, 7.9%), R290 (52.7 kW, 7.9%), and R1234yf (51.7 kW, 7.7%). Here, it should be noticed that other optimization conditions are almost the same (mass flow rate of the cold water 9.1–9.2 kg/s; performance of the condenser 91~92 kW/K) to get their maximum power output of ORC. In addition, it also known that low-GWP R1233zd (GWP: 1) can deserve the best option to replace R245fa (GWP: 950) and R1234yf (GWP: 4) also can replace r134a (GWP: 1430) since their optimization operation conditions are almost same.

1. Introduction

Energy shortage is one critical issue in this century that must be appropriately solved to realize a sustainable society. Utilization of low-temperature heat sources (lower than 100°C) to generate clean power is one promising way since its potential is huge. However, large amounts of the low-temperature heat sources are still not well-developed due to their relatively low thermal efficiencies and small power outputs.

Recently, researches on the conversion of the low-temperature heat sources into clean power have received a lot of attention, such as, geothermal energy conversion using Organic Rankine Cycle (ORC) (Hettiarachchiet al., 2007; Zhang et al., 2011; DiPippo, 2004; Sauret and Rowlands, 2011) and Kalina Cycle (Kalina and Leibowitz, 1989), ocean thermal energy conversion using ORC (Uehara and Ikegami, 1990; Wu, 1990; Uehara et al., 1998a; Ikegami and Bejan, 1998; Sun

et al., 2012a) using Kalina Cycle (Kalina, 1982, 1984) and Uehara Cycle (Uehara et al., 1998b), solar thermal power generation using ORC (Zhang et al., 2005; Wang et al., 2010; Delgado-Torres and Garcia-Rodriguez, 2010; Sun et al., 2013a) and Kalina Cycle (Lolos and Rogdakis, 2009; Sun et al., 2012b, 2013b, 2014; Wang et al., 2013), biothermal energy conversion using ORC (Liu et al., 2011), and waste heat power generation from various thermal processes using ORC (Hung et al., 1997; Liu et al., 2004; Wei et al., 2007; Dai et al., 2009) and Kalina Cycle (Kalina and Leibowitz, 1994; Fallah et al., 2016), etc. In which, the ORC technology is considered as one effective way since it has been installed throughout the world and the Rankine cycle provides most of worldwide electricity production.

ORC uses an organic fluid as the working fluid in Rankine cycle. The organic working fluids play a key role in ORC. Their suitable selection criteria are summarized for the conversion the low-temperature heat

* Corresponding author. College of Policy Science, Ritsumeikan University, 2-150 iwakura-cho, Ibaraki City, Osaka, 567-8570, Japan.

E-mail address: zhou@sps.ritsumei.ac.jp (W. Zhou).

<https://doi.org/10.1016/j.gerr.2024.100101>

Received 6 April 2024; Received in revised form 8 August 2024; Accepted 26 September 2024

2949-7205/© 2024 Published by Elsevier B.V. on behalf of Shandong University. This is an open access article under the CC BY-NC-ND license (<http://creativecommons.org/licenses/by-nc-nd/4.0/>).

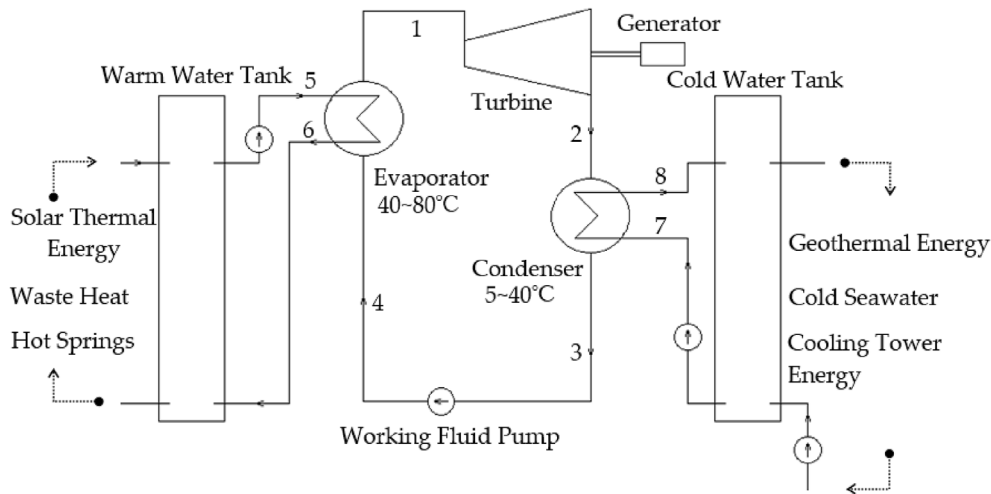


Fig. 1. The sketch of the ORC using Low-temperature Heat Sources.

sources and depending on the operating conditions (Saleh et al., 2007; Chen et al., 2010; Tchanche et al., 2011; Babatunde and Sunday, 2018; Herath et al., 2020; Yang et al., 2024), which is important for a particular application, i.e. solar thermal, geothermal or waste heat recovery, OTEC, etc. And isentropic fluids are considered the most suitable for recovering low-temperature waste heat (Hung et al., 1997). R134a high-density organic working fluid is favored for geothermal power generation from power output viewpoint (Sauret and Rowlands, 2011). R245fa is feasible and acceptable in the low-temperature solar power Rankine cycle system (Wang et al., 2010), and R1233zd and R245fa's net power outputs in ORC system are very close found by experimentally investigate (Araya et al., 2020). Ammonia (R717) is considered as one of the suitable working fluids for a closed Rankine cycle OTEC plant (Uehara et al., 1998a; Sun et al., 2012a).

In summary, although many studies described that ORC could be one possible way to convert low-temperature heat sources into electricity effectively. However, theoretical optimum operating parameters for maximum power generation of ORC and its contribution to generate green and zero-carbon energy are not given clearly. This work focuses on the theoretical analysis of some typical or low-GWP organic working fluids, such as R717, R134a, R1234yf, R290, R245fa and R1233zd, in ORC to get their optimization operation conditions directly to develop next generation green and zero-carbon energy generation system to promote the race to zero. Besides, results related to ORC system can also be applied in the marine industry for further high efficiency and lower emission in the future. Thus, this paper can be organized as follows:

- Modelling and methodology: details of the proposed method for the development of next-generation green and zero-carbon energy generation system to promote the race to zero are presented.

Table 1
Typical organic working fluids in ORC.

Working fluids	R717	R134a	R1234yf	R290	R245fa	R1233zd
Fluid type	Wet	Wet	Wet	Wet	Isentropic	Isentropic
Inflammability	Lower	No	Lower	Higher	No	No
Toxicity	Higher	Lower	Lower	Lower	Lower	Lower
Metal corrodibility	Higher	No	No	No	No	No
ODP	0	0	0	0	0	0
GWP (100 years)	<1	1430	4	3	950	1
Market	Easy	Difficult in the future	Easy	Easy	Difficult in the future	Easy
Availability						

- Results and discussion: results of the proposed method and analysis of the theoretical optimization operation conditions for maximum power generation are described and provided.
- Conclusion and future work: contributions of the paper, limitations of the proposed method, and potential directions for future research are summarized and suggested.

2. ORC Modelling for power generation from low-temperature heat sources

ORC is named for its use of organic working fluids, which allows Rankine cycle to generate electricity from Low-temperature Heat Sources. A sketch of the ORC is shown in Fig. 1.

Some typical working fluids (Table 1), such as R717, R134a, R1234yf, Propane (R290), R245fa and R1233zd, are selected and their practical issues like environmental-friendly (ozone depletion potential (ODP), global warming potential (GWP)), safety use (toxicity, flammability, corrodibility) and the market availability are also given for reference. From a thermodynamics point of view, the selected working fluids can be classified as “wet” (e.g., R717, R134a, R1234yf and R290), and “isentropic” (e.g., R245fa and R1233zd) depending on the slope of the saturation vapor curve on a temperature-entropy diagram. Figs. 2 and 3 show the ORC on the temperature-entropy plane by using “wet” and “isentropic” working fluid, respectively.

Thermodynamic performance of these working fluids in ORC can be evaluated by the following theoretical analysis. State function of every point in ORC are defined in Table 2. And the corresponding coefficient values are shown in Table 3 for these working fluids (R717, R134a, R245fa, R1233zd, R1234yf, and R290).

In ORC (Fig. 1), the net power output can be given as (turbine, pump):

$$\dot{W}_{net} = \dot{W}_t - \dot{W}_p \tag{1}$$

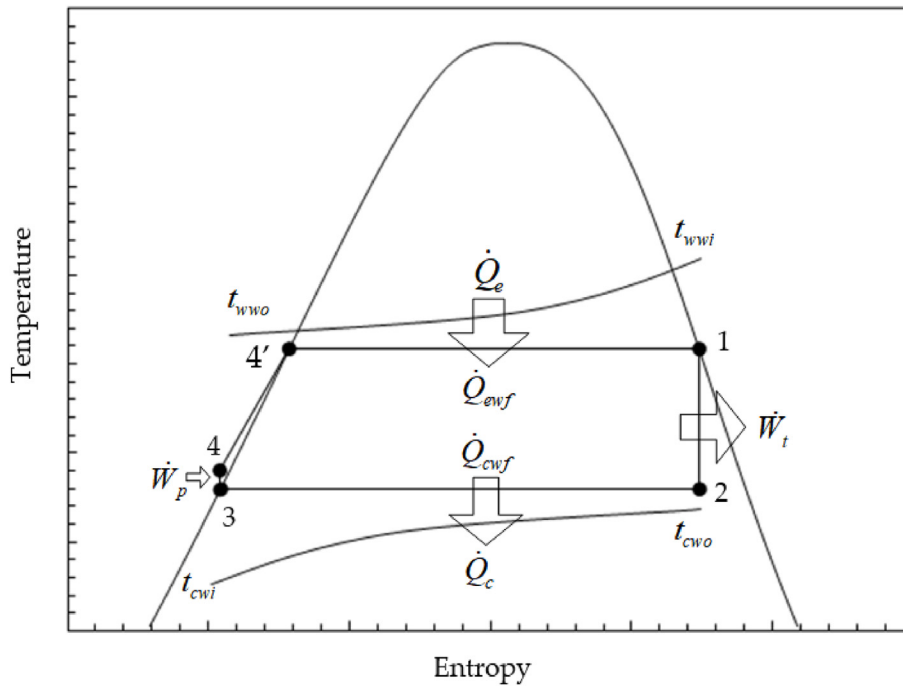


Fig. 2. Temperature-entropy for “wet” working fluids.

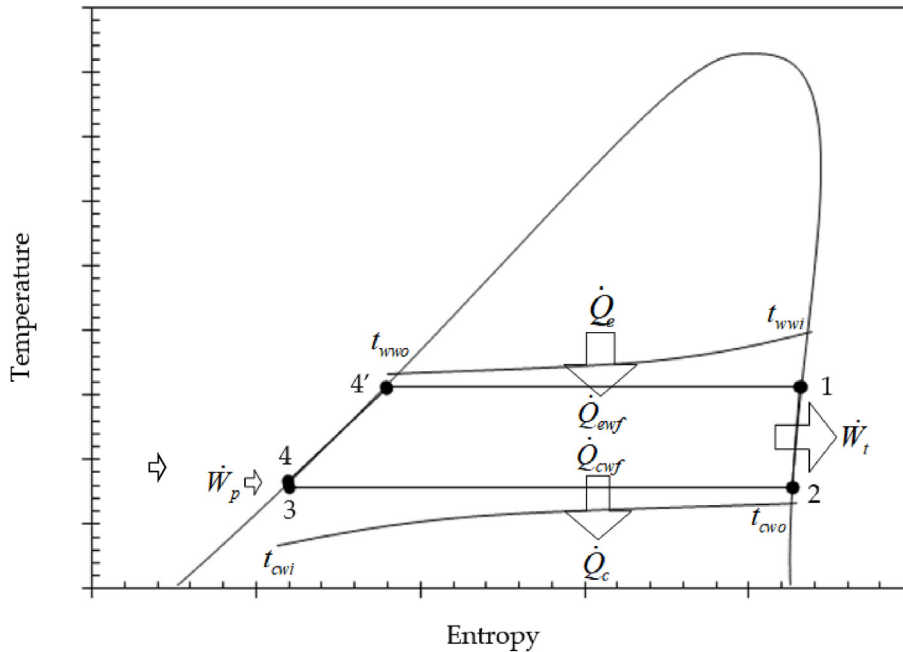


Fig. 3. Temperature-entropy for “isentropic” working fluids.

where $\dot{W}_t = \dot{m}_{wf} (h_1 - h_2)$ is the gross power output in the turbine, $\dot{W}_p = \dot{m}_{wf} (h_4 - h_3)$ represents the power consumed in the pump, \dot{m}_{wf} is the mass flow rate of working fluid.

In the evaporator of ORC, the heat balance can be given as (evaporator):

$$\dot{Q}_c = \dot{Q}_{cwf} \quad (2)$$

where, $\dot{Q}_e = \dot{m}_{ww} c_p \Delta t_{ww}$ is the heat transfer rate absorbed from the warm-water, $\dot{Q}_{ewf} = \dot{m}_{wf} (h_1 - h_4)$ is the heat transfer rate supplied to the cycle, \dot{m}_{ww} is the mass flow rate of warm water, c_p represents the specific heat

capacity for water in a constant pressure system, $\Delta t_{ww} = t_{wwi} - t_{wwo}$, t_{wwi} and t_{wwo} are respectively the warm-water temperature at the inlet and outlet of the evaporator.

In the condenser of ORC, the heat balance can be given as (condenser):

$$\dot{Q}_c = \dot{Q}_{cwf} \quad (3)$$

where, $\dot{Q}_c = \dot{m}_{cw} c_p \Delta t_{cw}$ is the heat transfer rate rejected into the cold-water, $\dot{Q}_{cwf} = \dot{m}_{wf} (h_2 - h_3)$ is the heat transfer rate rejected from the cycle, \dot{m}_{cw} is the mass flow rate of cold water, $\Delta t_{cw} = t_{cwo} - t_{cwi}$, t_{cwi} and t_{cwo} are the cold-water temperature at the inlet and outlet of the condenser.

Table 2
State function of every point in ORC.

Point	State	Items	Equations
0	Zero celsius degree	Absolute temperature [K]	$T_0 = 273.15$
1	Saturated vapor	Enthalpy [kJ/kg] Pressure [kPa] Entropy [kJ/(kg·K)]	$h_1 = \zeta_{h_1,1} t_e^2 + \zeta_{h_1,2} t_e + \zeta_{h_1,3}$ $P_1 = \zeta_{P_1,1} t_e^2 + \zeta_{P_1,2} t_e + \zeta_{P_1,3}$ $s_1 = \zeta_{s_1,1} t_e^2 + \zeta_{s_1,2} t_e + \zeta_{s_1,3}$
2	Wet vapor	Enthalpy [kJ/kg] Pressure [kPa] Entropy [kJ/(kg·K)]	$h_2 = h_3 + (t_e + T_0) \cdot (s_2 - s_3)$ $P_2 = P_3$ $s_2 = s_1$
3	Saturated liquid	Enthalpy [kJ/kg] Pressure [kPa] Entropy [kJ/(kg·K)] Specific volume [m ³ /kg]	$h_3 = \zeta_{h_3,1} t_e^2 + \zeta_{h_3,2} t_e + \zeta_{h_3,3}$ $P_3 = \zeta_{P_3,1} t_e^2 + \zeta_{P_3,2} t_e + \zeta_{P_3,3}$ $s_3 = \zeta_{s_3,1} t_e^2 + \zeta_{s_3,2} t_e + \zeta_{s_3,3}$ $v_3 = \zeta_{v_3}$
4	Compressed liquid	Enthalpy [kJ/kg] Entropy [kJ/(kg·K)] Pressure [kPa]	$h_4 = h_3 + v_3(P_1 + P_3)$ $s_4 = s_3$ $P_4 = P_1$

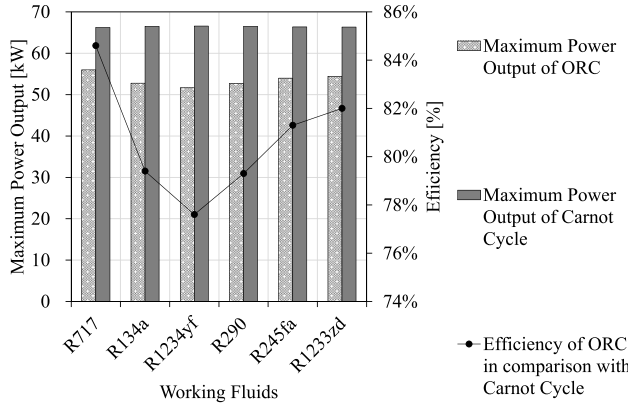


Fig. 4. Comparison of different working fluids on ORC in terms of maximum power output and efficiency in comparison with Carnot cycle.

In addition, the heat transfer rate between energy resources and working fluid can also be given (evaporator, condenser):

$$\dot{Q} = UA\Delta T_m \quad (4)$$

where, U is the overall heat-transfer coefficient, A is the cross-section area normal to the direction of heat transfer, $\Delta T_m = (\Delta t_i - \Delta t_o) / \ln(\Delta t_i / \Delta t_o)$ is called the logarithmic mean temperature difference (LMTD), Δt_i represents the temperature difference of heat exchanger end section (heat source inlet), Δt_o shows the temperature difference of heat exchanger end section (heat source outlet). Thus, according to the energy balance at the evaporation, evaporation temperature of the evaporator can be given as

$$t_e = t_{wwi} - \left(t_{wwi} \cdot \exp \left[\frac{(UA)_e}{\dot{m}_{ww} c_p} \right] / 1 - \exp \left[\frac{(UA)_e}{\dot{m}_{ww} c_p} \right] \right) \quad (5)$$

Thus, according to Eqs. (1)–(5), the \dot{W}_{net} can be written as,

$$\dot{W}_{net} = \dot{m}_{ww} c_p \cdot \left(t_{wwi} - \frac{t_{wwi} - t_e (1 - \exp[\alpha])}{\exp[\alpha]} \right) \left(1 - \frac{A(t_c, t_e)}{B(t_c, t_e)} \right) \quad (6)$$

where it is used to calculate the net power output of ORC from the heat transfer rate absorbed from the warm-water and ORC's performance (thermal efficiency), and where, $t_c = (t_{cwi} - (t_{cwi} + t_{wwi} - (t_{wwi} - t_e \cdot (1 - \exp[\alpha])) / \exp[\alpha]) \cdot \exp[\beta]) / (1 - \exp[\beta])$, $40^\circ\text{C} \leq t_e \leq 80^\circ\text{C}$, $5^\circ\text{C} \leq t_c \leq 40^\circ\text{C}$, $\alpha = (UA)_e / (\dot{m}_{ww} c_p)$, $\beta = (UA)_c / (\dot{m}_{ww} c_p \cdot A(t_c, t_e) / B(t_c, t_e))$

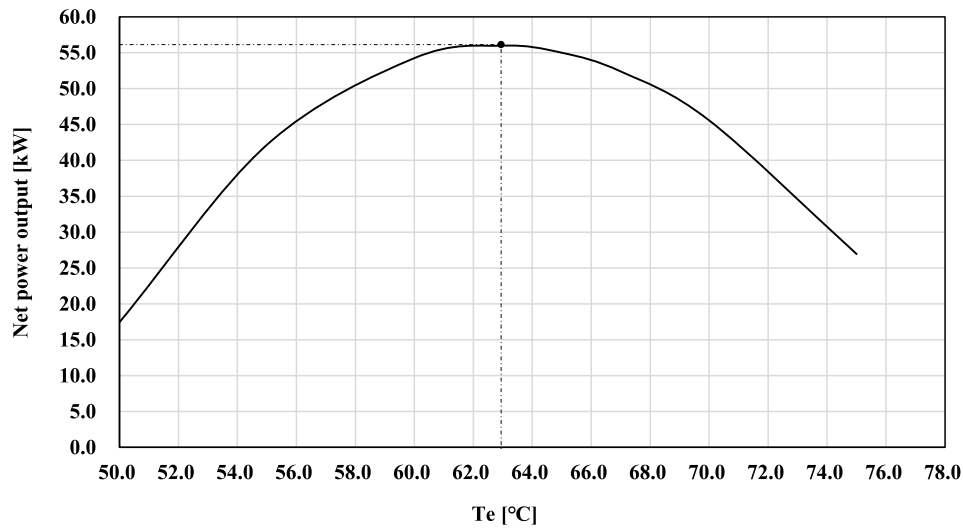


Fig. 5. Relationship between t_e and \dot{W}_{net} with same initial conditions of R717 shown in Table 6.

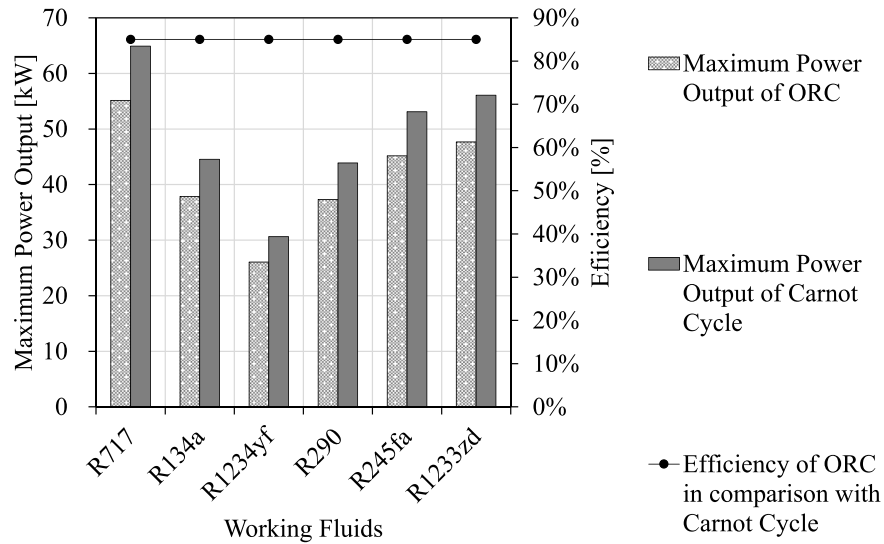


Fig. 6. Comparison of different working fluids on ORC in terms of maximum power output with the same efficiency of ORC in comparison with Carnot cycle.

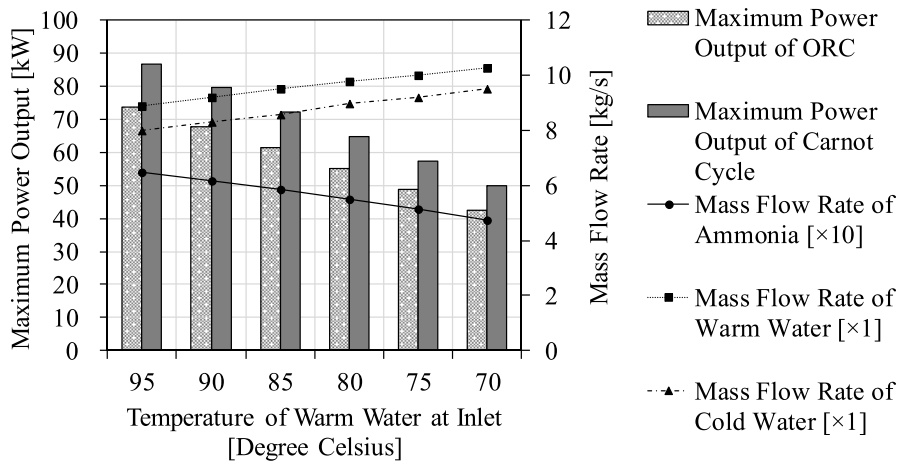


Fig. 7. Influence of t_{wwi} on the R717 ORC in terms of maximum power output with the same efficiency in comparison with Carnot cycle.

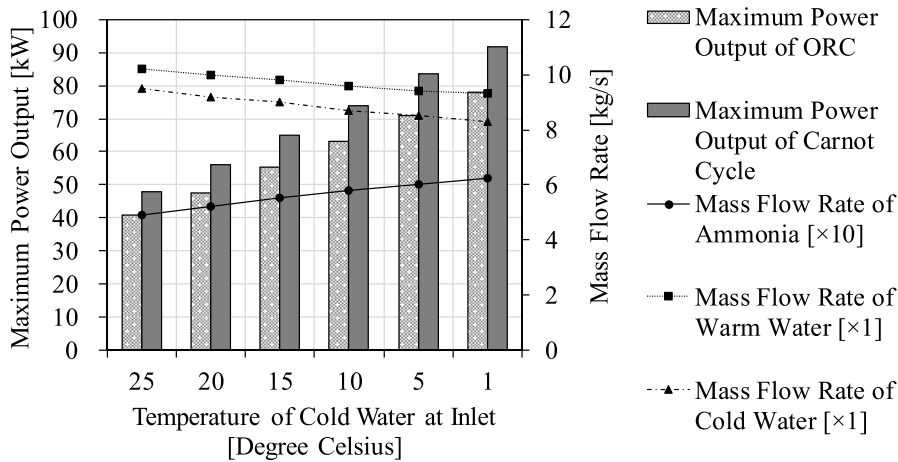


Fig. 8. Influence of t_{cwi} on the R717 ORC in terms of maximum power output with the same efficiency in comparison with Carnot cycle.

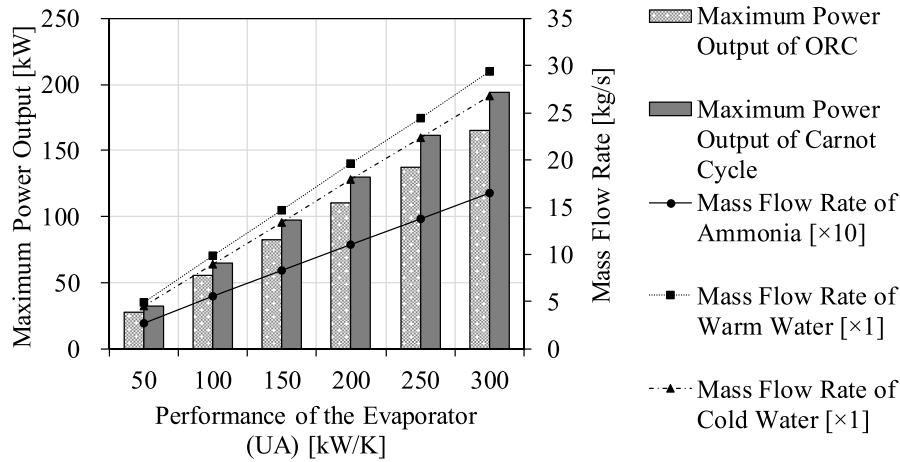


Fig. 9. Influence of $(UA)_e$ on the R717 ORC in terms of maximum power output with the same efficiency in comparison with Carnot cycle.

t_e), $A(t_c, t_e) = (t_c + T_0) \cdot (a_1 t_c^2 + a_2 t_e^2 + a_3 t_e + a_4 t_c + a_5)$, $B(t_c, t_e) = b_1 t_c^2 + b_2 t_e^2 + b_3 t_e + b_4 t_c + b_5$.

To get the maximum net power output of ORC theoretically, the theoretical optimization design (Table 4) is used to solve Eq. (6) as below.

$$\begin{aligned} & \max \{ \dot{W}_{net} \}_{orc} \\ & = \dot{m}_{ww} c_p \left(t_{wwi} - \frac{t_{wwi} - (t_e)_{opt} (1 - \exp[\alpha])}{\exp[\alpha]} \right) \left(1 - \frac{A((t_c)_{opt}, (t_e)_{opt})}{B((t_c)_{opt}, (t_e)_{opt})} \right) \end{aligned} \quad (7)$$

In the expression,

$$\begin{aligned} A((t_c)_{opt}, (t_e)_{opt}) &= ((t_c)_{opt} + T_0) \\ &\cdot (a_1 (t_c)_{opt}^2 + a_2 (t_e)_{opt}^2 + a_3 (t_e)_{opt} + a_4 (t_c)_{opt} + a_5) \end{aligned} \quad (8)$$

$$B((t_c)_{opt}, (t_e)_{opt}) = b_1 (t_c)_{opt}^2 + b_2 (t_e)_{opt}^2 + b_3 (t_e)_{opt} + b_4 (t_c)_{opt} + b_5 \quad (9)$$

where, $a_i (i = 1, \dots, 5)$, $b_i (i = 1, \dots, 5)$ and $c_i (i = 1, \dots, 6)$ are constant coefficients, varied with working fluid medium. Such as R717, R134a, R245fa, R1233zd, R1234yf, and R290, whose corresponding coefficient values are shown in Table 5.

Thus, it is easy to know that $\max \{ \dot{W}_{net} \}_{orc}$ depends on the performance of the evaporator $((UA)_e)$ and heat capacity at constant pressure (c_p) as well as the warm and cold-water temperature at the inlet, t_{wwi} , t_{cwi} and mass flow rate of warm water \dot{m}_{ww} .

Meanwhile, the following optimal operation condition values can also be given as follows, in which, Eq. (11), (12) and (14) derived from energy balance at the condensation and Eq. (13) derived from the turbine' heat transfer rate supplied to the cycle.

$$t_{wwo} = \frac{t_{wwi} - (t_e)_{opt} \cdot (1 - \exp[\alpha])}{\exp[\alpha]} \quad (10)$$

$$t_{cwo} = t_{cwi} + t_{wwi} - t_{wwo} \quad (11)$$

$$\dot{m}_{cw} = \dot{m}_{ww} \cdot \frac{A((t_c)_{opt}, (t_e)_{opt})}{B((t_c)_{opt}, (t_e)_{opt})} \quad (12)$$

$$\dot{m}_{wf} = \frac{\max \{ \dot{W}_{net} \}_{orc}}{h_1((t_c)_{opt}) - h_2((t_c)_{opt}, (t_e)_{opt})} \quad (13)$$

Table 3
Constant coefficients of organic fluids for the state function of every point in ORC.

Working fluids	R717	R134a	R1234yf	R290	R245fa	R1233zd
$\zeta_{h1,1}$	-1.7876e-02	-6.2410e-03	-7.1811e-03	-1.4624e-02	-7.6592e-04	-8.9258e-04
$\zeta_{h1,2}$	1.7698	9.9516e-01	1.1714	2.1504	7.9390e-01	7.6816e-01
$\zeta_{h1,3}$	1590.6051	389.4105	351.5388	551.0576	403.1600	403.7864
$\zeta_{h3,1}$	3.9878e-03	1.9118e-03	2.1823e-03	5.0082e-03	1.0747e-03	4.6113e-04
$\zeta_{h3,2}$	4.6020	1.3317	1.2838	2.4736	1.2706	1.2224
$\zeta_{h3,3}$	343.2888	200.0629	200.0424	200.1463	200.0204	200.0223
$\zeta_{s1,1}$	-2.9320e-06	-1.0923e-05	-1.5180e-05	-2.8389e-05	1.9682e-06	1.5652e-06
$\zeta_{s1,2}$	-1.0115e-02	6.9016e-04	1.6491e-03	1.9731e-03	3.2470e-04	2.2104e-04
$\zeta_{s1,3}$	6.0349	1.7004	1.5651	2.3050	1.7412	1.7435
$\zeta_{s3,1}$	-1.5799e-05	-2.2528e-06	-1.1332e-06	-1.2300e-08	-4.1033e-06	-5.7227e-06
$\zeta_{s3,2}$	1.6726e-02	4.8447e-03	4.6694e-03	8.9698e-03	4.6347e-03	4.4533-03
$\zeta_{s3,3}$	1.4722	1.0002	1.0001	1.0005	1.0001	1.0002
$\zeta_{p1,1}$	5.8267e-01	3.5765e-01	3.1744e-01	3.3461e-01	1.4323e-01	1.1423e-01
$\zeta_{p1,2}$	-5.5589	-2.7089	-7.4941e-01	3.7371	-3.8044	-2.7190
$\zeta_{p1,3}$	851.4715	556.6621	543.9449	687.8062	175.1930	142.8210
$\zeta_{p3,1}$	3.5071e-01	2.1524e-01	1.9500e-01	2.1998e-01	7.6177e-02	6.2164e-02
$\zeta_{p3,2}$	13.7436	9.2652	9.5793	13.3971	1.7860	1.6218
$\zeta_{p3,3}$	441.3651	299.7510	321.6670	480.0812	56.2418	50.4481
ζ_{v3}	1.6510e-03	8.2412e-04	9.1066e-04	2.0200e-03	7.4396e-04	7.8872e-04

Table 4
Constant coefficients of the state function of every point in ORC for power generation from Low-temperature heat sources.

Steps	Optimization Details
Step1	Design variable $X = \begin{pmatrix} t_e \\ t_c \end{pmatrix}$ Find $\max_{t_e, t_c} \{ \dot{W}_{net}(X) \}$ Satisfy $g_1(X) = t_e - 40 \geq 0, g_2(X) = 80 - t_e \geq 0,$ $g_3(X) = t_c - 5 \geq 0, g_4(X) = 40 - t_c \geq 0.$ $f_1(X) =$ $\frac{t_{cwi} - (t_{cwi} + t_{wwi} - (t_{wwi} - t_e \cdot (1 - \exp[\alpha])) / \exp[\alpha]) \cdot \exp[\beta]}{1 - \exp[\beta]} - t_c = 0$ (energy balance at the condensation)
⇓	
Step2	Penalty Function $F(X) = \frac{1}{\dot{W}_{net}(X)} + R_k (f_1(X))^2 + \gamma_k \sum_{j=1}^4 \frac{1}{g_j(X)}$ Find $\min_{t_e, t_c, \gamma_k \rightarrow 0, R_k \rightarrow \infty} \{ F(X) \}$ Assume $40^\circ C \leq (t_e)_{opt} \leq 80^\circ C, 5^\circ C \leq (t_c)_{opt} \leq 40^\circ C$ Solve $f_1(X) = 0 \Leftrightarrow \begin{cases} (t_e)_{opt} = (t_{cwi} + t_{wwi}) - (t_c)_{opt} \\ (UA)_c = (UA)_e \cdot \frac{A((t_c)_{opt}, (t_e)_{opt})}{B((t_c)_{opt}, (t_e)_{opt})} \\ \Delta t_{ww} = \Delta t_{cw} \\ \dot{m}_{cw} = \dot{m}_{ww} \cdot \frac{A((t_c)_{opt}, (t_e)_{opt})}{B((t_c)_{opt}, (t_e)_{opt})} \end{cases}$
⇓	
Step3	Find $\max_{t_e} \{ \dot{W}_{net}(t_e) \}$ Solve $(t_e)_{opt} = c_1 t_{cwi}^2 + c_2 t_{wwi} \cdot t_{cwi} + c_3 t_{wwi}^2 + c_4 t_{cwi} + c_5 t_{wwi} + c_6$ $(t_e)_{opt} = -c_1 t_{cwi}^2 - c_2 t_{wwi} \cdot t_{cwi} - c_3 t_{wwi}^2 + (1 - c_4) t_{cwi} + (1 - c_5) t_{wwi} - c_6$
⇓	
Result	$\max \{ \dot{W}_{net} \}_{orc} = \dot{m}_{ww} c_p \cdot \left(t_{wwi} - \frac{t_{wwi} - (t_e)_{opt} (1 - \exp[\alpha])}{\exp[\alpha]} \right) \left(1 - \frac{A((t_c)_{opt}, (t_e)_{opt})}{B((t_c)_{opt}, (t_e)_{opt})} \right)$

$$(UA)_c = (UA)_e \cdot \frac{A((t_c)_{opt}, (t_e)_{opt})}{B((t_c)_{opt}, (t_e)_{opt})} \tag{14}$$

Meanwhile, the corresponding ORC thermal efficiency at maximum net power output is

$$\eta_{orc} = 1 - \frac{A((t_c)_{opt}, (t_e)_{opt})}{B((t_c)_{opt}, (t_e)_{opt})} \tag{15}$$

From this equation, ORC thermal efficiency for maximum net power output is only decided by the warm and cold-water temperature at the inlet, t_{wwi} and t_{cwi} , for a given working fluid.

The potential net power output of the ORC or maximum power output of Carnot cycle (Ikegami and Bejan, 1998) is

$$\dot{W}_{carnot} = \frac{(\sqrt{t_{wwi} + T_0} - \sqrt{t_{cwi} + T_0})^2}{(\dot{m}_{ww} c_p)^{-1} + (\dot{m}_{cw} c_p)^{-1}} \tag{16}$$

The efficiency of ORC in comparison with the Carnot cycle is

$$\eta_{orc, carnot} = \frac{\max \{ \dot{W}_{net} \}_{orc}}{\dot{W}_{carnot}} \times 100\% \tag{17}$$

which is defined by comparing the ORC with the Carnot cycle in terms of the maximum net power output. In this way, the parameter can be used to

Table 5
Constant coefficients of organic fluids to get the maximum net power output in ORC.

Coefficients		1	2	3	4	5	6
R717	a_i	1.5799e-05	-2.9320e-06	-1.0115e-02	-1.6726e-02	4.5627	-
	b_i	-3.4088e-03	-1.8838e-02	1.7789	-4.5793	1246.6393	-
	c_i	1.7755e-04	3.7940e-04	2.0663e-04	7.4895e-01	2.5004e-01	6.2668e-02
R134a	a_i	2.2528e-06	-1.0923e-05	6.9016e-04	-4.8447e-03	7.0017e-01	-
	b_i	-1.7344e-03	-6.5358e-03	9.9740e-01	-1.3241	189.1358	-
	c_i	1.3316e-04	-6.2219e-04	2.2385e-04	7.6058e-01	2.6402e-01	-7.1341e-01
R-1234yf	a_i	1.1332e-06	-1.5180e-05	1.6491e-03	-4.6694e-03	5.6500e-01	-
	b_i	-2.005e-03	-7.4702e-03	1.1720	-1.2751	151.2940	-
	c_i	9.6429e-05	-7.2092e-04	1.9362e-04	7.6739e-01	2.7468e-01	-1.1829
R290	a_i	1.2300e-08	-2.8389e-05	1.9731e-03	-8.9698e-03	1.3045	-
	b_i	-4.5639e-03	-1.5300e-02	2.1428	-2.4465	350.4918	-
	c_i	1.1020e-04	-6.6237e-04	2.0319e-04	7.6476e-01	2.6920e-01	-9.6838e-01
R245fa	a_i	4.1033e-06	1.9682e-06	3.2470e-04	-4.6347e-03	7.4107e-01	-
	b_i	-1.0181e-03	-8.7248e-04	7.9673e-01	-1.2693	203.0510	-
	c_i	1.7296e-04	-3.9031e-04	2.5408e-04	7.4516e-01	2.4800e-01	8.1594e-02
R1233zd	a_i	5.7227e-06	1.5652e-06	2.2104e-04	-4.4533e-03	7.4337e-01	-
	b_i	-4.1210e-04	-9.8267e-04	7.7030e-01	-1.2212	203.6913	-
	c_i	1.5612e-04	-3.9490e-04	2.3342e-04	7.4630e-01	2.4951e-01	3.5570e-02

Table 6
Initial conditions and performance comparison of different working fluids on ORC.

	R717	R134a	R1234yf	R290	R245fa	R1233zd
t_{wvi} [°C]	80					
t_{wwo} [°C]	64.5	64.1	63.9	64.1	64.3	64.3
t_{cwi} [°C]	15					
t_{cwo} [°C]	30.5	30.9	31.1	30.9	30.7	30.7
$t_{e,opt}$ [°C]	62.9	62.5	62.3	62.4	62.7	62.8
$t_{c,opt}$ [°C]	32.1	32.5	32.7	32.6	32.3	32.2
$P_{e,opt}$ [MPa]	2.808	1.783	1.729	2.225	0.500	0.422
$P_{c,opt}$ [MPa]	1.243	0.829	0.843	1.150	0.193	0.167
\dot{m}_{ww} [kg/s]	10					
\dot{m}_{cw} [kg/s]	9.1	9.2	9.2	9.2	9.2	9.2
\dot{m}_{wf} [kg/s]	0.560	3.499	4.164	1.821	3.135	3.119
$Q_{wf,l}$ [L/min]	56.8	173	227.5	220.7	139.9	150.3
η_{orc} [%]	8.6%	7.9%	7.7%	7.9%	8.2%	8.3%
$(UA)_c$ [kW/K]	100					
$(UA)_c$ [kW/K]	91	92	92	92	92	92
$max\{\dot{W}_{net}\}_{orc}$ [kW]	56.0	52.8	51.7	52.7	54.0	54.4
\dot{W}_{carnot} [kW]	66.2	66.5	66.6	66.5	66.4	66.4
$\eta_{orc,carnot}$ [%]	84.6%	79.4%	77.6%	79.3%	81.3%	82.0%

evaluate the designed ORC system is efficient or not. And the rest part ($1 - \eta_{orc,carnot}$) implies the energy loss of the ORC.

3. Results and discussion

It is known that suitable working fluid can make ORC get better performance in terms of more power generation and higher efficiency from low-temperature heat sources. Fig. 4 shows the effect and comparison of different working fluids on ORC with the same initial conditions as shown in Table 6. Meanwhile, the parameters of temperature of the warm water at outlet of the evaporator (t_{wwo}), temperature of the cold water at outlet of the condenser (t_{cwo}), mass flow rate of the cold water (\dot{m}_{cw}), mass flow rate of the working fluid (\dot{m}_{wf}), and performance of the condenser ($(UA)_c$) can be given by using equations 10–14. And corresponding state of every point on ORC is given in Table 7.

Results show that, for the same initial conditions, such as, $t_{wvi} = 80^\circ\text{C}$, $t_{cwi} = 15^\circ\text{C}$, $\dot{m}_{ww} = 10\text{ kg/s}$, and $(UA)_e = 100\text{ kW/K}$, R717 has the best performance in terms of the maximum power output ($max\{\dot{W}_{net}\}_{orc} = 56.0\text{ kW}$) with thermal efficiency of 8.6% (η_{orc}), and the next is the R1233zd, it is 54.4 kW ($max\{\dot{W}_{net}\}_{orc}$) with thermal efficiency of 8.3% (η_{orc}). And Fig. 5 display the relationship between t_e and \dot{W}_{net} with same initial conditions of R717 shown in Table 6. The $t_{e,opt} = 62.9^\circ\text{C}$ and corresponding to $max\{\dot{W}_{net}\}_{orc,R717} = 56.0[\text{kW}]$ match very

Table 7
State of every point for different working fluids on ORC.

Point	Items	R717	R134a	R1234yf	R290	R245fa	R1233zd
1	Enthalpy [kJ/kg]	1631.3	427.3	396.7	628.4	449.9	448.5
	Pressure [MPa]	2.808	1.783	1.729	2.225	0.500	0.422
	Entropy [kJ/(kg·K)]	5.387	1.701	1.609	2.318	1.769	1.764
	Temperature [°C]	62.9	62.5	62.3	62.4	62.7	62.8
2	Enthalpy [kJ/kg]	1531.3	412.1	384.3	599.5	432.7	431.0
	Pressure [MPa]	1.243	0.829	0.843	1.150	0.193	0.167
	Entropy [kJ/(kg·K)]	5.387	1.701	1.609	2.318	1.769	1.764
	Temperature [°C]	32.1	32.5	32.7	32.6	32.3	32.2
3	Enthalpy [kJ/kg]	495.1	245.4	244.3	286.1	242.2	239.9
	Pressure [MPa]	1.243	0.829	0.843	1.150	0.193	0.167
	Entropy [kJ/(kg·K)]	1.993	1.155	1.152	1.293	1.146	1.138
	Temperature [°C]	32.1	32.5	32.7	32.6	32.3	32.2
4'	Enthalpy [kJ/kg]	650.3	427.3	289.3	376.0	284.1	448.5
	Pressure [MPa]	2.808	1.783	1.729	2.225	0.500	0.422
	Entropy [kJ/(kg·K)]	2.468	1.701	1.289	1.566	1.276	1.764
	Temperature [°C]	62.9	62.5	62.3	62.4	62.7	62.8
4	Enthalpy [kJ/kg]	501.9	247.6	246.8	293.1	242.7	240.3
	Pressure [MPa]	2.808	1.783	1.729	2.225	0.500	0.422
	Entropy [kJ/(kg·K)]	1.993	1.155	1.152	1.293	1.146	1.138
	Temperature [°C]	32.5	33.1	33.4	33.5	32.4	32.3

Table 8
Initial conditions and performance comparison of different working fluids on ORC with the same efficiency in comparison with Carnot cycle.

	R717	R134a	R1234yf	R290	R245fa	R1233zd
t_{wvi} [°C]	80					
t_{wwo} [°C]	64.4	63.0	62.4	62.9	63.6	63.8
t_{cwi} [°C]	15					
t_{cwo} [°C]	30.6	32.0	32.6	32.1	31.4	31.2
$t_{e,opt}$ [°C]	62.9	62.5	62.3	62.4	62.7	62.8
$t_{c,opt}$ [°C]	32.1	32.5	32.7	32.6	32.3	32.2
$P_{e,opt}$ [MPa]	2.808	1.783	1.729	2.225	0.500	0.422
$P_{c,opt}$ [MPa]	1.243	0.829	0.843	1.150	0.193	0.167
\dot{m}_{ww} [kg/s]	9.8	6.7	4.6	6.6	8	8.5
\dot{m}_{cw} [kg/s]	9.0	6.2	4.2	6.1	7.3	7.8
\dot{m}_{wf} [kg/s]	0.551	2.509	2.099	1.289	2.622	2.728
$Q_{wf,l}$ [L/min]	55.9	124.1	114.7	156.2	117.0	131.6
η_{orc} [%]	8.6%	7.9%	7.7%	7.9%	8.2%	8.3%
$(UA)_c$ [kW/K]	100					
$(UA)_c$ [kW/K]	91	92	92	92	92	92
$max\{\dot{W}_{net}\}_{orc}$ [kW]	55.2	37.9	26.0	37.3	45.2	47.6
\dot{W}_{carnot} [kW]	64.9	44.6	30.6	43.9	53.1	56.0
$\eta_{orc,carnot}$ [%]	85.0%					

well with equations of Table 4, which indicates that the solution for theoretical optimization result of maximum power output in ORC is correct. Here, it should be noticed that other optimization conditions are almost the same to get the maximum power output of ORC, such as, $\dot{m}_{cw} = 9.1 \sim 9.2\text{ kg/s}$, $(UA)_c = 91 \sim 92\text{ kW/K}$. In this case, mass flow rate, volumetric flow rate of the working fluid, saturation pressure of the evaporator and saturation pressure of the condenser are noticeable different between them, such as, $\dot{m}_{wf,R717} = 0.560\text{ kg/s}$, $\dot{m}_{wf,R1233zd} = 3.119\text{ kg/s}$; $\nu_{wf,R717} = 56.8\text{ L/min}$, $\nu_{wf,R1233zd} = 150.3\text{ L/min}$; $P_{e,opt,R717} = 2.808\text{ MPa}$, $P_{e,opt,R1233zd} = 0.422\text{ MPa}$; $P_{c,opt,R717} = 1.243\text{ MPa}$, $P_{c,opt,R1233zd} = 0.167\text{ MPa}$. It means that R1233zd needs a larger piping system in ORC than R717. However, the pressure-resistant standard of R717 ORC system is higher than R1233zd ORC system since the working pressure of R717 is noticeably higher than that of R1233zd.

From the optimized results as shown in Table 6, we also know that R1233zd (GWP: 1) can deserve the best option to replace R245fa (GWP: 950) on the condition of maximum net power output in ORC, because it is not only a non-ozone depleting, low global warming potential (GWP) HFO refrigerant (Table 1), but also a suitable replacement working fluid for R245fa for maximizing net power output with the same initial conditions and almost the same optimization conditions (Table 6), such as, $t_{wvi} = 80^\circ\text{C}$, $t_{cwi} = 15^\circ\text{C}$, $\dot{m}_{ww} = 10\text{ kg/s}$, $\dot{m}_{cw} = 9.2\text{ kg/s}$,

$(UA)_e = 100 \text{ kW/K}$, $(UA)_c = 92 \text{ kW/K}$, $\dot{m}_{wf} = 3.119 \sim 3.135 \text{ kg/s}$, $\nu_{wf} = 139.9 \sim 150.3 \text{ L/min}$, $P_{e,opt} = 0.422 \sim 0.500 \text{ MPa}$, $P_{c,opt} = 0.167 \sim 0.193 \text{ MPa}$. In this case, their maximum net power outputs are respectively $\max \{\dot{W}_{net}\}_{orc,R1233zd} = 54.4 \text{ kW}$ and $\max \{\dot{W}_{net}\}_{orc,R245fa} = 54.0 \text{ kW}$, which shows that R1233zd and R245fa's net power outputs are very close and coincides with Araya's experimentally investigate (Araya et al., 2020). And it also means that the proposed model is correct. In same, R1234yf (GWP: 4) also can replace r134a (GWP: 1430) since their optimization operation conditions are almost same.

For comparison, potential net power output of ORC (maximum power output of the Carnot cycle) and the potential efficiency of the ORC are also shown in Fig. 4 and Table 6. It shows that the maximum power output of the Carnot cycle with these working fluids (R717, R134a, R1234yf, R290, R245fa, R1233zd) are almost the same ($\dot{W}_{carnot} = 66.2 \sim 66.6 \text{ kW}$).

Meanwhile, the efficiency of ORC ($\eta_{orc,carnot}$) in comparison with the Carnot cycle varies with the working fluid is given here, such as R717 $\eta_{orc,carnot,R717} = 84.6\%$ is the highest, the next one is R1233zd $\eta_{orc,carnot,R1233zd} = 82.0\%$ and R1234yf $\eta_{orc,carnot,R1234yf} = 77.6\%$ is the lowest, etc.

Furthermore, the efficiency of ORC in comparison with Carnot cycle is kept constant for working fluids comparison, such as 85.0% as shown in Fig. 6 and Table 8, by adjusting the mass flow rate of the warm water (\dot{m}_{ww}). It shows the same result in comparison with the maximum power output of these working fluids, R717 is the largest, the next is the R1233zd, the following is the R245fa, and the last is the R1234yf. However, the maximum power output of the designed ORC system in R717 is 55.2 kW, R1233zd is 47.7 kW, R245fa is 45.2 kW, and the last is R1234yf (26.0 kW).

In this way, if the R1234yf ORC system is designed to have the same efficiency of ORC and the same maximum power output with the R717 ORC system, the scale of the heat exchangers in R1234yf ORC system ($(UA)_{e,c}$) should be enlarged enough, which results in an increase in initial capital investment of the ORC system.

Moreover, R717 ORC is discussed in more detail as below. Effect of different low-temperature heat sources (less than 100 C), such as the temperature of warm water at the inlet $t_{wwi} = 70 \sim 90^\circ\text{C}$ to the maximum power output of ORC ($\max \{\dot{W}_{net}\}_{orc,R717}$) is shown in Fig. 7. Effect of different cold sources, such as the temperature of cold water at the inlet $t_{cwi} = 25 \sim 1^\circ\text{C}$ to $\max \{\dot{W}_{net}\}_{orc,R717}$ is shown in Fig. 8. And effect of performance of the evaporator $(UA)_e = 50 \sim 300 \text{ kW/K}$ to $\max \{\dot{W}_{net}\}_{orc,R717}$ is shown in Fig. 9.

It is clear that $\max \{\dot{W}_{net}\}_{orc,R717}$ is nearly linearly increased with increasing of the temperature of warm water at inlet (t_{wwi}) or performance of the evaporator $(UA)_e$ and is linearly decreased with increasing of the temperature of cold water at inlet t_{cwi} with same efficiency of ORC in comparison with Carnot cycle, such as $\eta_{orc,carnot} = 85.0\%$, which can be realized by adjusting the operating parameter of the mass flow rate of the warm, cold water and the working fluid ($\dot{m}_{ww}, \dot{m}_{cw}, \dot{m}_{wf}$) with the aid of the proposed theoretical optimum model. Meanwhile, it is shown that about 6 kW of the maximum power output can be increased by increasing the t_{wwi} for 5°C , about 7 ~ 8 kW of the maximum power output can be increased by decreasing 5°C of t_{cwi} , and about 28 kW of the maximum power output can be increased by increasing the performance of the evaporator by 50 kW/K for $(UA)_e$. In addition, the others optimal operating conditions, such as the temperature of warm water at the outlet (t_{wwo}), the temperature of cold water at the outlet (t_{cwo}) can be given by using equations 10 and 11, and $(UA)_c$ can be given by equation (14). And the optimal rate of $(UA)_c$ to $(UA)_e$ is almost the same $(UA)_c / (UA)_e = 0.91 \sim 0.92[-]$ since the corresponding ORC thermal efficiency is about 8 ~ 9%. Thus, from the initial conditions of t_{wwi} and t_{cwi} , for example $t_{wwi} = 85^\circ\text{C}$ and $t_{cwi} = 15^\circ\text{C}$ are fixed, the optimal ORC can be designed directly, and its maximum power output is 82.6 kW for $(UA)_e = 150 \text{ kW/K}$ with optimal operation condition of $\dot{m}_{ww} = 14.7[\text{kg/s}]$, $\dot{m}_{cw} =$

$13.4[\text{kg/s}]$, $\dot{m}_{wf} = 0.825[\text{kg/s}]$ and $(UA)_c = 137 \text{ kW/K}$. In the way, theoretical optimum model with its optimal operating parameters for maximum power generation of ORC and its contribution to generate green and zero-carbon energy by using some typical or low-GWP organic working fluids can be given clearly.

4. Conclusions

Theoretical analysis of some typical or low-GWP organic working fluids in ORC for maximum power generation is studied for development of green and zero-carbon energy generation system to promote the race to zero. Results show that this study provides a theoretical basis for the design of ORC to optimization with getting their optimization operation conditions, which also will favor the design and optimization for green marine industry (marine waste-heat recovery, ocean thermal energy conversion, etc.). Thus, following results can be given:

1. Temperatures of warm and cold water at inlet, mass flow rate of the warm water and performance of the evaporator play a key role for maximum power generation. And the corresponding thermal efficiency could be evaluated using the temperatures of warm and cold water at inlet.
2. In the case of the same initial conditions of temperatures of warm water (85°C) and cold water (15°C) at the inlet, the mass flow rate of the warm water (10 kg/s) and performance of the evaporator (100 kW/K), R717 has the best performance in terms of the maximum power output 56.0 kW with thermal efficiency of 8.6%, and the next is the R1233zd (54.4 kW, 8.3%), R245fa (54.0 kW, 8.2%), R134a (52.8 kW, 7.9%), R290 (52.7 kW, 7.9%), and R1234yf (51.7 kW, 7.7%). Here, it should be noticed that other optimization conditions are almost the same (mass flow rate of the cold water 9.1~9.2 kg/s; performance of the condenser 91~92 kW/K) to get their maximum power output of ORC.
3. Low-GWP R1233zd (GWP: 1) can deserve the best option to replace R245fa (GWP: 950) and R1234yf (GWP: 4) also can replace r134a (GWP: 1430) since their optimization operation conditions are almost same.
4. Potential net power output of ORC with these working fluids are almost the same. Meanwhile, efficiency of ORC in comparison with the Carnot cycle varies with the working fluid, R717 is the highest, the next one is R1233zd. In addition, in the case of keeping efficiency of ORC as constant for comparison maximum power output of these working fluids in ORC by adjusting mass flow rate of the warm water, it shows the same result, R717 is the largest, the next is the R1233zd.
5. Theoretical optimum model with its operating parameters for design maximum power generation of ORC and its contribution to generating green and zero-carbon energy by using some typical or low-GWP organic working fluids is given clearly.

It should be noticed that the proposed model is suitable for low-temperature heat sources, in the future, we will enhance and enlarge its applicability to medium-temperature heat sources to make it more effective since ORC technology is currently one of the most efficient ways to turn medium and low temperature heat energy into electric power.

CRediT authorship contribution statement

Baoju Jia: Writing – review & editing, Writing – original draft. **Yu Lei:** Writing – review & editing. **Faming Sun:** Writing – review & editing. **Weisheng Zhou:** Writing – review & editing.

Declaration of competing interest

We declare that we have no financial and personal relationships with other people or organizations that can inappropriately influence our

work, there is no professional or other personal interest of any nature or kind in any product, service and/or company that could be construed as influencing the position presented in, or the review of, the manuscript entitled, "Theoretical analysis of organic Rankine cycle for maximum power generation in optimization operation conditions".

References

- Araya, S., Wemhoff, A., Jones, G., Fleischer, A., 2020. An experimental study of an Organic Rankine Cycle utilizing HCFO-1233zd (E) as a drop-in replacement for HFC-245fa for ultra-low-grade waste heat recovery. *Appl. Therm. Eng.* 180, 115757.
- Babatunde, A., Sunday, O., 2018. A review of working fluids for organic rankine cycle (ORC) applications. *IOP Conf. Ser. Mater. Sci. Eng.* 413, 012019.
- Chen, H.J., Goswami, D.Y., Stefanakos, E.K., 2010. A review of thermodynamic cycles and working fluids for the conversion of low-temperature heat. *Renew. Sustain. Energy Rev.* 14 (9), 3059–3067.
- Dai, Y.P., Wang, J.F., Gao, L., 2009. Parametric optimization and comparative study of organic Rankine cycle (ORC) for low-temperature waste heat recovery. *Energy Convers. Manag.* 50 (3), 576–582.
- Delgado-Torres, A.M., Garcia-Rodriguez, L., 2010. Analysis and optimization of the low-temperature solar organic Rankine cycle (ORC). *Energy Convers. Manag.* 51 (12), 2846–2856.
- DiPippo, R., 2004. Second Law assessment of binary plants generating power from low-temperature geothermal fluids. *Geothermics* 33, 565–586.
- Fallah, M., Mohammad, S., Mahmoudi, S., Yari, M., Akbarpour Ghiasi, R., 2016. Advanced exergy analysis of the Kalina cycle applied for low temperature enhanced geothermal system. *Energy Convers. Manag.* 108, 190–201.
- Herath, H., Wijewardane, M., Ranasinghe, R., Jayasekera, J., 2020. Working fluid selection of organic rankine cycles. *Energy Rep.* 6 (9), 680–686.
- Hettiarachchi, H.D.M., Golubovica, M., Worek, W.M., Ikegami, Y., 2007. Optimum design criteria for an Organic Rankine cycle using low-temperature geothermal heat sources. *Energy* 32 (9), 1698–1706.
- Hung, T.C., Shai, T.Y., Wang, S.K., 1997. A review of organic rankine cycles (ORCs) for the recovery of low-temperature waste heat. *Energy* 22 (7), 661–667.
- Ikegami, Y., Bejan, A., 1998. On the thermodynamic optimization of power plants with heat transfer and fluid flow irreversibilities. *J. Sol. Energy Eng.* 120, 139–144.
- Kalina, A.I., 1982. Generation of Energy by Means of a Working Fluid, and Regeneration of a Working Fluid. United States: N.
- Kalina, A.I., 1984. Combined-cycle system with a novel bottoming cycle. *J. Eng. Gas Turbines Power* 106, 737–742.
- Kalina, A.I., Leibowitz, H.M., 1989. Application of the Kalina cycle technology to geothermal power generation. *Geothermal Resources Council Proceedings* 13, 605–611.
- Kalina, A.I., Leibowitz, H.M., 1994. Applying Kalina Cycle technology to high enthalpy geothermal resources. *Trans. Geoth. Resour. Council.* 18, 531–536.
- Liu, B.T., Chien, K.H., Wang, C.C., 2004. Effect of working fluids on organic Rankine cycle for waste heat recovery. *Energy* 29 (8), 1207–1217.
- Liu, H., Shao, Y.J., Li, J.X., 2011. A biomass-fired micro-scale CHP system with organic Rankine cycle (ORC)-Thermodynamic modelling studies. *Biomass Bioenergy* 35 (9), 3985–3994.
- Lolos, P.A., Rogdakis, E.D., 2009. A Kalina power cycle driven by renewable energy sources. *Energy* 34 (4), 457–464.
- Saleh, B., Koglbauer, G., Wendland, M., Fischer, J., 2007. Working fluids for low-temperature organic Rankine cycles. *Energy* 32 (7), 1210–1221.
- Sauret, E., Rowlands, A.S., 2011. Candidate radial-inflow turbines and high-density working fluids for geothermal power systems. *Energy* 36 (7), 4460–4467.
- Sun, F.M., Ikegami, Y., Jia, B.J., Arima, H., 2012a. Optimization design and exergy analysis of organic Rankine cycle in ocean thermal energy conversion. *Appl. Ocean Res.* 35, 38–46.
- Sun, F.M., Ikegami, Y., Jia, B.J., 2012b. A study on Kalina solar system with an auxiliary superheater. *Renew. Energy* 41, 210–219.
- Sun, F.M., Ikegami, Y., Arima, H., Zhou, W.S., 2013a. Performance analysis of the low temperature solar-boosted power generation system e part I: comparison between Kalina solar system and Rankine solar system. *J. Sol. Energy Eng.* 135, 1–11, 011006.
- Sun, F.M., Ikegami, Y., Arima, H., Zhou, W.S., 2013b. Performance analysis of the low temperature solar-boosted power generation system e part II: thermodynamic characteristics of the Kalina solar system. *J. Sol. Energy Eng.* 135, 1–8, 011007.
- Sun, F.M., Zhou, W.S., Ikegami, Y., Nakagami, K., Su, X.M., 2014. Energy-exergy analysis and optimization of the solar-boosted Kalina cycle system 11 (KCS-11). *Renew. Energy* 66, 268–279.
- Tchanche, B.F., Lambrinos, G., Frangoudakis, A., Papadakis, G., 2011. Low-temperature heat conversion into power using organic Rankine cycles – a review of various applications. *Renew. Sustain. Energy Rev.* 15 (8), 3963–3979.
- Uehara, H., Ikegami, Y., 1990. Optimization of a closed-cycle OTEC system. *J. Sol. Energy Eng.* 112, 247–256.
- Uehara, H., Dilao, C.O., Nakaoka, T., 1998a. Conceptual design of ocean thermal energy conversion power plants in the Philippines. *Sol. Energy* 41 (5), 431–441.
- Uehara, H., Ikegami, Y., Nishida, T., 1998b. Performance analysis of OTEC system using a cycle with absorption and extraction processes. *Transactions of the Japan Society of Mechanical Engineers (Part B)* 64, 384–389.
- Wang, X.D., Zhao, L., Wang, J.L., Zhang, W.Z., Zhao, X.Z., Wu, W., 2010. Performance evaluation of a low-temperature solar rankine cycle system utilizing R245fa. *Sol. Energy* 84 (3), 353–364.
- Wang, J.F., Yan, Z.Q., Zhou, E.M., Dai, Y.P., 2013. Parametric analysis and optimization of a Kalina cycle driven by solar energy. *Appl. Therm. Eng.* 50 (1), 408–415.
- Wei, D.H., Lu, X.S., Lu, Z., 2007. Performance analysis and optimization of organic Rankine cycle (ORC) for waste heat recovery. *Energy Convers. Manag.* 48 (4), 1113–1119.
- Wu, C., 1990. Specific power optimization of closed-cycle OTEC plants. *Ocean Eng.* 17 (3), 307–314.
- Yang, M., Liu, M., Yeh, R., 2024. Investigation of low-GWP working fluids as substitutes for R245fa in organic Rankine cycle application. *Heliyon* 10, e34219.
- Zhang, X.R., Yamaguchi, H., Fujima, K., Enomoto, M., Sawada, N., 2005. A feasibility study of CO₂-based Rankine cycle powered by solar energy. *JSME Int. J. Ser. B Fluids Therm. Eng.* 48, 540–547.
- Zhang, S.J., Wang, H.X., Guo, T., 2011. Performance comparison and parametric optimization of subcritical Organic Rankine Cycle (ORC) and transcritical power cycle system for low-temperature geothermal power generation. *Appl. Energy* 88 (8), 2740–2754.